Journal of Engineering and Sustainable Development
Vol. 29, No. 05, August 2025
https://jeasd.uomustansiriyah.edu.iq/index.php/jeasd
ISSN 2520-0917
Research Article
https://doi.org/10.31272/jeasd.2498

Performance Enhancement of Double-Pass Solar Air Heater Using Phase Change Materials and Air Flow Turbulators

Zainab Nadeem Suzah*, Ahmed J. Hamad, Abdul Hadi N. Khalifa

Department of Mechanical Power Engineering, Middle Technical University. Baghdad, Iraq

*Corresponding Email: abc0042@mtu.edu.iq

Article Info

Received	**13/03/2024**
Revised	**04/08/2025**
Accepted	**04/08/2025**

Abstract

In this study, two techniques to improve the thermal performance of the double-pass solar air heater are experimentally investigated. The first is integrating a phase change material (PCM) as a thermal storage system, and the second is using flow turbulators with the absorber plate to enhance the heat transfer in the solar air heater (SAH). Four different arrangements of the modified SAH absorber plate, integrated with and without PCM and flow turbulators, with longitudinal fins on the plate's lower surface, are investigated. The modified SAH was examined based on three air flow rates, 0.002, 0.005, and 0.012 kg/s, under the climatic conditions of Baghdad city. The results demonstrated that the modified double-pass SAH integrated with PCM outperformed the conventional SAH. The outlet air temperature in modified cases 1, 2, and 3 was higher by about 22, 14, and 9%, respectively, compared with the conventional case of a flat plate. The V-shaped flow turbulator revealed optimal performance, with an improvement in thermal efficiency of 35%, compared with 26% and 19% for cases 1 and 2, respectively. It was observed that the use of PCM increased the operating time by 2 hours after sunset.

Keywords: Energy saving, Flow turbulators, Phase change material, Solar heater, Thermal performance.

1. Introduction

World population growth and its material needs increase energy requirements every year. On the other hand, the use of fossil fuels for energy production leads to environmental degradation. Therefore, the world turned to using renewable energy sources for energy production to meet the energy shortage. Solar energy is one of the most important sources of renewable energy, which is free, available, endless, and environmentally friendly [1]-[3]. The most common way to invest in solar energy is by converting it into thermal energy through the use of solar collector systems such as solar air heater (SAH). A solar air heater is a device that absorbs solar radiation as a renewable source of energy and converts it into thermal energy to heat the air passing through the heater channel. A conventional SAH consists of an absorber plate, air channel, air fan, glass cover, and thermally insulated structure. The function of the solar air heater (SAH) is to absorb the heat energy of solar radiation and release it to the air through heat exchange between the absorber plate and the air. The efficiency of the conventional SAH (single pass) can be improved by using a double pass for airflow, which will extend the heat transfer surface area and then enhance the heat transfer process in the SAH. Solar air heater is used in many applications such as space heating, drying crops, desalinating water, and other applications. The use of solar air heaters to accomplish these operations leads to reduced operational costs and reduces the consumption of traditional energy sources.

Conventional air heaters usually have low efficiency due to increased thermal resistance and a low heat transfer coefficient. An improvement can be made on the heat transfer rate by creating increased turbulence in the air flow field. Much work has been carried out worldwide to evaluate the performance and use of various optimization techniques for different types of solar air heaters [4], [5]. Rajendran et al. [6] conducted an experimental study to improve the performance of SAH by adding V-shaped perforated baffles at different values of air mass flow rate with and without baffles. It was found that the highest thermal efficiency was 89.3% at an air flow rate of 0.0346 kg/s, which was 13% higher than in the case without baffles. Kumar et al. [7] investigated double-pass solar air collectors to improve their performance by using a V-corrugation winglet with different arrangements. It was observed that the highest thermal efficiency was 49.5% at an air mass flow rate of 0.02 kg/s. In addition, increasing the air flow rate from 0.01 kg/s to 0.02 kg/s increased the pressure drop inside the collector. The researchers Kumar et al. [8] and Bekele et al. [9] used artificial roughness represented by delta shape obstacles to study the effect of the length of the space between shapes and the effect of increasing turbulence on improving heat transfer. The results showed that when the space between the shapes decreases, the air turbulence increases, indicating the effectiveness of obstacles in enhancing the heat transfer of SAH. Rajaseenivasan et al. [10] studied experimentally the effect of using circular and V-type flow turbulators fixed on the absorber plate for six different cases with Reynolds numbers (6000-12000). It was noticed that the efficiency of SAHs increased by increasing the Reynolds number and the number of flow turbulators. Furthermore, the maximum outlet temperature of the air was 66 °C at an airflow rate of 57.7 when a V-type was used inside the circular tube. Pandey and Kumar [11] fabricated a solar air heater with a V-baffle perforated at an angle of 45 ° and distributed in a staggered arrangement above and below the absorber surface to improve heat transfer. The results proved that the staggered arrangement method enhanced the heat transfer, and the highest thermal efficiency was 96.6% at Re = 13021. To preserve the environment, Yaseen et al. [12] used metal cans as flow turbulators by reusing them inside a double-pass solar air heater. It was observed that the surface area for heat transfer increased, and the maximum efficiency was 75.9% at a temperature difference of 21 °C during the experiment. Abdullah et al. [13] investigated the effect of placing an external mirror to increase the solar radiation falling on the SAH and using aluminum cans as flow turbulators. The results revealed a daily efficiency of 73% at an air flow rate of 0.05 kg/s. Many research works [14]-[16] examined effective procedures to improve the performance of SAH by using phase change material (PCM) such as paraffin wax placed inside a container or capsules, and benefit from it during sunset periods. During their experimental works, the researchers demonstrated an improvement and increase in the outlet temperature of air and an increase in the daily efficiency of SAH. Ali et al. [17] conducted an experimental study for a double pass solar air heater in the conditions under Baghdad city. Metal tubes filled with paraffin wax were used to evaluate the charging and discharging characteristics for different days in the winter season at different flow rate values (0.025-0.06) kg/s. The greatest efficiency was 90% and 61% at 0.04 kg/s with and without PCM, respectively. Abdelkader et al. [18] evaluated energy and exergy of a solar collector with the use of arc-shaped ribs. The authors concluded that the increase in efficiency when using the ribs was 18.8% higher than that for the smooth plate. Alabdeen et al. [19] investigated experimentally the thermal performance of SAH with different arrangements of delta turbulators. These turbulators were used for vortex generation and damping development of the thermal boundary layer, in the direction of air flow, and increased energy conservation. Hussein et al. [20] studied the effect of replacing the traditional absorber plate of SAHs with a tubular solar absorber filled with water as a phase change material. The longitudinal tubular proved effective to produce hot air, and the efficiency reached 80.9% at an air flow rate of 0.03 kg/s. The researchers [21]-[27] investigated various shapes to create turbulence in the airflow field, represented by baffles, fins, ribs, obstacles, and various flow turbulators to improve the heat transfer in SAHs. Several studies were conducted by the researchers [28], [29] to improve the thermal efficiency of SAH by increasing the heat load using different techniques such as artificial roughness, V-grooves, obstructions, or fins on the absorber surface. Based on the previous literature, it can be concluded that the thermal efficiency of SAH can be significantly improved by creating a turbulence effect in the air flow field to enhance the heat transfer rate. In addition, incorporating thermal storage systems with SAHs has proven effective in developing SAH performance. Low thermal performance represents one of the SAH disadvantages; thus, many developments are required to improve its efficiency. Therefore, in the present work, two techniques to improve the thermal performance of the double-pass SAH are experimentally investigated. The first is integrating a phase change material (PCM) as a thermal storage system, and the second is using flow turbulators with the absorber plate to enhance the heat transfer in the SAH. The current study aims to enhance the thermal performance of conventional SAH by incorporating PCM and flow turbulators of different shapes on the upper surface of the absorber plate and longitudinal fins on the plate's lower surface. Different effective parameters on SAH thermal performance, such as air flow rate, flow turbulator shape, air outlet temperature, energy saving, and thermal efficiency, were studied to determine their effects on the thermal performance of modified SAH. Experimental work was conducted under Baghdad city (latitude 33°19′ N, longitude 44°25′ E) climatic conditions in February and March at various operating conditions.

2. Materials and Methods

2.1. Experimental Setup

The experimental work was conducted using a test rig for a double-pass solar air heater integrated with PCM, as shown in Figs. Figs. 1 and 2. The solar air heater consisted of outer structure fabricated from Aluminum sheets of thickness 0.09 cm and size of (90 x 40 x 14) cm^3 with two openings for air entry and exit of area (40 x 6) cm^2 as illustrated in Fig.3. The SAH is thermally insulated from the sides and bottom using glass wool (k = 0.038 W/m.ºC, and 4 cm thickness) for reducing the heat loss to the surrounding and covered by 0.4 cm thick glass sheet at the top. The PCM container of size (80 x 40 x 2) cm^3 was fabricated from 0.09 cm-thick Aluminum sheets and filled with 6 kg of paraffin wax as PCM. The upper surface of the PCM container, which is subjected to solar radiation, represents the absorber plate of the SAH and is painted black. While the lower surface of the container was equipped with five longitudinal fins of 5mm thickness Aluminum sheet equally distributed along the container surface to enhance the heat exchange between entering air and SAH absorber plate as shown in Fig.1. The air is supplied to SAH at flowrate 0.002–0.012 kg/s using centrifugal air fan of 27.5W capacity, model AKS 680–180 with power regulator placed at the SAH air outlet opening. The SAH test rig was equipped with measuring devices; K-type thermocouples in the range of -200 to 1250 ºC with a digital reader fixed at different locations in the SAH air flow channel and PCM container, three thermocouples at the absorber plate, five inside the PCM container, one at the air channel inlet, and one at the air channel outlet. The air velocity through the air channel was measured using a digital anemometer (Am802), and the pressure drop in the SAH air channel was measured using an adjustable slope manometer at an angle of 15 °15 °. The solar irradiance was recorded using a solar irradiance meter of model (TES1333) with a measuring range of 100–1250 W/m^2.The thermophysical properties of PCM used in the current study are illustrated in Table 1.

2.2. Air Flow Turbulators

To modify the conventional solar air heater, air flow turbulators with different geometries are fabricated and installed on the SAH absorber plate in the present study. Integrating air flow turbulators with the absorber plate can create turbulence in the air flow through the SAH channel, thereby enhancing heat exchange and improving SAH thermal performance. Three different geometrical shapes of air flow turbulators, namely, V-shape, vertical cylindrical, and horizontal cylindrical, are manufactured and welded in staggered arrangement on the absorber plate of the SAH as shown in Figs. 4 and 5. The air flow turbulators are constructed using Aluminum sheets and tubes with approximately equal dimensions, as illustrated in Table 2.

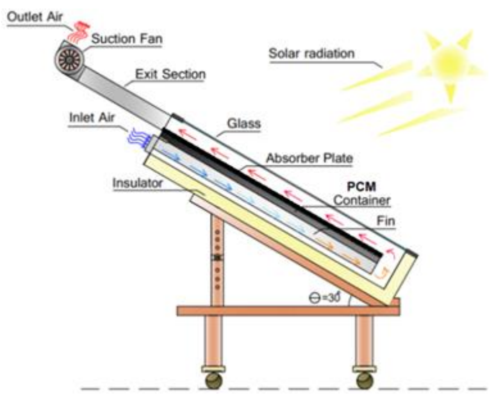

Figure 1. A schematic of a conventional double-pass solar air heater (SAH).

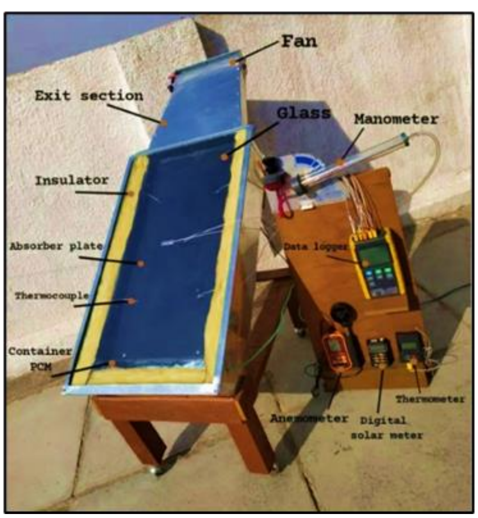

Figure 2. Double pass solar air heater with measurement devices.

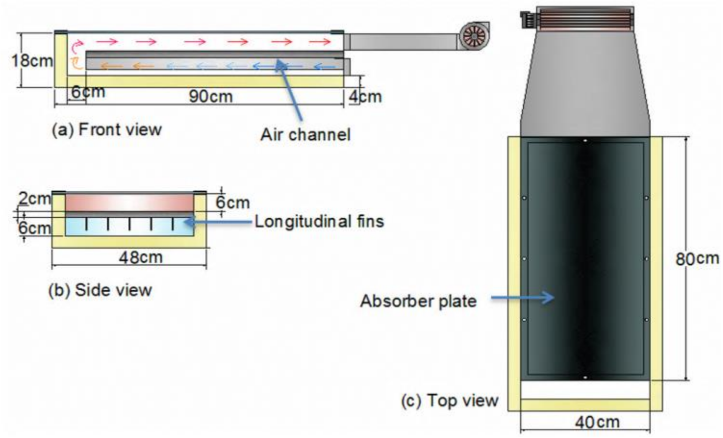

Figure 3. Dimensions of SAH: (a) air channel, (b) absorber plate.

Table 1. Thermophysical properties of PCM [30].

Properties	PCM (Paraffin Wax)
Melting temperature	52-54 ºC
Thermal conductivity	0.4 W/m.ºC (liquid)
	0.34 W/m.ºC(solid)
Density	890 kg/m^3 (liquid)
	910 kg/m^3 (solid)
Specific heat capacity	4 kJ/kg.ºC (liquid)
	3 kJ/kg.ºC (solid)
Latent heat of fusion	230 kJ/kg

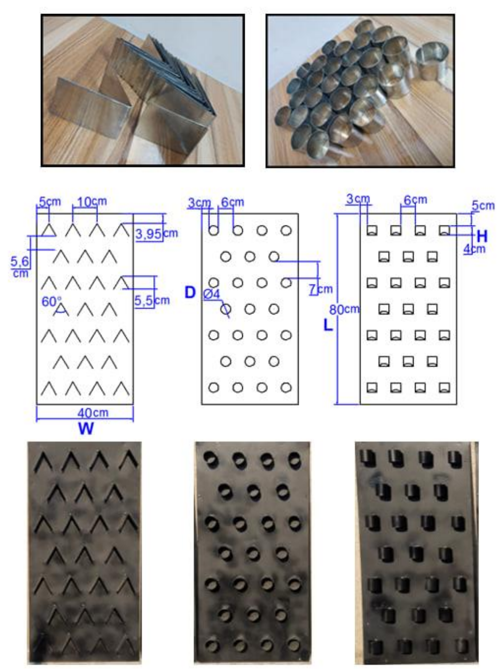

Figure 4. Distribution and dimensions of air flow turbulators installed on the absorber plate.

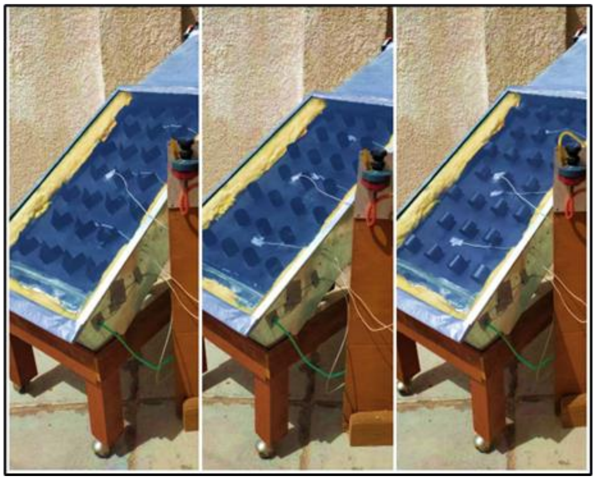

Figure 5. Solar air heater with air flow turbulators.

Table 2. Dimensions of air flow turbulators.

Cases	Geometry	Dimension
Case1	V-shape	L=6.3cm, H=4cm, θ= 60°
Case2	Circular shape-vertical	H=4cm, D=4cm
Case3	Circular shape-horizontal	H=4cm, D=4cm

2.3. Experimental Methodology

The experimental tests are conducted in February and March 2023 during sunshine hours from 9.00 am to 4.00 pm under Baghdad city (latitude 33°19′ N, longitude 44°25′ E) climatic conditions. To face the solar radiation, the SAH was installed on a wooden stand at an angle of 30 ° with the horizontal and directed to the southwest.

Four testing cases of SAH with and without PCM and flow turbulators are experimentally investigated as illustrated in Table 3 and Fig.6. After preparing the SAH test rig and connecting the thermocouples and measuring devices properly, the SAH system was turned on 10 minutes before recording the measurements to ensure all devices were working properly. The air fan speed was regulated to ensure the specified air mass flow rates of 0.002, 0.005, and 0.012 kg/s. In the first case (base case) without flow turbulators and PCM (flat absorber plate), at air flow rate 0.002 kg/s, the readings of absorber plate, PCM, and air temperatures, solar radiation, and outlet air speed at a time interval of 30 minutes during a testing period from 9.00 am to 4.00 pm are monitored and recorded. These steps are repeated for air flow rates of 0.005 and 0.012 kg/s with PCM, and for other test cases 1, 2, and 3 without and with air flow turbulators and PCM.

2.4. Data Reduction

The sound heat energy supplied to the air by the solar air heater due to the heat exchange between the absorber plate and the air can be determined as follows [31],[13]:

$$Q_u = \dot{m}_a \, C_{pa} \, (T_{out} - T_{in}) \qquad (1)$$

The mass flow rate of the air flowing in the SAH channel, $\dot{m}_a$, was calculated by:

$$\dot{m}_a = \rho_a \, \nu_a \, A_c \qquad (2)$$

Where:

A_c: cross-sectional area of the SAH air channel (m^2).

C_{pa}: air specific heat (J/kg. s).

T_{in}: air inlet temperature (°C).

T_{out}: air outlet temperature (°C)

ρ_a: air density (kg/m^3)

ν_a: air velocity in the SAH channel (m/s).

Disregard the heat losses to the surroundings and the heat stored by the absorber plate; the rate of heat (Q_{pcm}) transferred to the PCM during a sunshine period can be determined by: [30]:

$$Q_{pcm} = F_r \,.(\alpha.\, \tau.\, G.\, A_s - (h.\, A_s.\, (T_s\text{-}T_{in}) \qquad (3)$$

The heat transfer coefficient h (W/m^2.°C) of the SAH absorber plate can be determined experimentally from Eq. (4):

$$h = \frac{Q_u}{A_s.(T_s - T_{in})} \qquad (4)$$

Where, A_s is the SAH absorber plate surface area (m^2), T_s is the absorber plate temperature, and G is the solar irradiance (W/m^2), and:

F_r: heat removal factor for the collector

α: absorptivity of the absorber plate

τ: transmissivity of the collector glass cover

The values of the factors F_r, τ, and α are approximated to 0.9, 0.85, and 0.9, respectively [32].

Table 3. Testing cases are considered in the present experimental work.

Cases	Geometry	Air flow rate (kg/s)
Base Case	With & Without PCM Flat Plate	
Case-1	V-Shape	$\dot{m}_1$=0.002 $\dot{m}_2$=0.005 $\dot{m}_3$=0.012
Case-2	Cylindrical shape (vertical position)	
Case-3	Cylindrical shape (Horizontal position)	

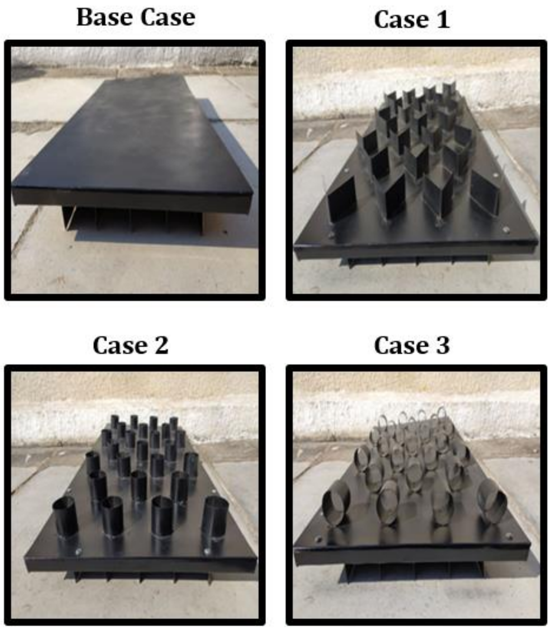

Figure 6. Testing cases of the SAH absorber plate with flow turbulators.

The charging time (t_{ch}) during the PCM melting process through a sunshine period (s) and PCM mass (m_{pcm}) can be estimated by (5) [29]:

$$m_{pcm}.L_{pcm} + q_{sen} = Q_{pcm}.t_{ch} \qquad (5)$$

The heat energy (J) stored by PCM during the charging cycle (melting process) at the excess heat energy period through sunshine hours represents the energy saving (Q_{sav}) by PCM and can be estimated by:

$$Q_{sav} = q_{lat}.f_{lq} + q_{sen} \qquad (6)$$

Where L_{pcm} represents the PCM latent heat of fusion (J/kg), q_{lat} and q_{sen} are the PCM latent heat and sensible heat (J) of the PCM, respectively, which can be determined as follows:

$$q_{lat} = m_{pcm}.L_{pcm} \qquad (7)$$

$$q_{sen} = m_{pcm}.Cp_{pcm}.(T_{lq} - \mathrm{T_{ml}}) \qquad (8)$$

Where $\mathrm{T_{ml}}$ is the PCM melting point temperature, and f_{lq} is the liquid fraction of PCM, which can be estimated by [33]:

$$f_{lq} = 0 \text{ if } T_{pcm} < \mathrm{T_{sd}} \qquad (9a)$$

$$f_{lq} = 1 \text{ if } T_{pcm} > \mathrm{T_{lq}} \qquad (9b)$$

$$f_{lq} = \frac{(T_{pcm} - \mathrm{T_{sd}})}{(T_{lq} - \mathrm{T_{sd}})} \text{ if } \mathrm{T_{sd}} < T_{pcm} < \mathrm{T_{lq}} \qquad (9c)$$

Where T_{pcm} is the PCM temperature at the specified time, T_{sd} is the solid PCM temperature when the last liquid content is solidified, and T_{lq} is the liquid PCM temperature when the previous solid content is liquefied.

Through a relatively low solar radiation period, the heat stored in the PCM is released to the air passing through the SAH channel during the time (t_{ds}) at the discharging cycle (PCM solidification process) can be expressed by Eq. (10):

$$\dot{m}_a.C_{pa}.(T_{set} - T_{in}).\ t_{ds} = q_{lat}.f_{lq} + q_{sen} \qquad (10)$$

The desired set point air temperature (T_{set}) for building heating purposes is approximated in the range of (35–40 °C) [34].

The thermal efficiency of the solar air heater (η_{th}) can be expressed by:

$$\eta_{th} = \frac{Q_u}{\alpha.\tau.G.A_{S.}}.100\% \qquad (11)$$

2.5. Uncertainty Analysis

An error analysis was conducted to ensure the accuracy of the measurements for the present experimental work. The uncertainty in the measurements is determined based on the method reported in Coleman [35].

Assume (R) is a function of independent variables *x1, x2, ..., xn*. Thus, the measurements are used to calculate some results, R in the experiment:

$$R=R(x_1, x_2, x_3 \ldots, xn) \qquad (12)$$

Let W_1, W_2, W_3 …Wn represent the uncertainties in the independent variables. Therefore, the uncertainty in the results (W_R) can be expressed by:

$$W_R = \left[\left(\frac{\partial R}{\partial X_1} W_1\right)^2 + \left(\frac{\partial R}{\partial X_2} W_2\right)^2 + \cdots + \left(\frac{\partial R}{\partial X_i} W_n\right)^2\right]^{\frac{1}{2}} \qquad (13)$$

For a thermal efficiency η_{th} from equation (11), if A_b, Cp, and α. If τ is assumed to be a constant, it can be concluded that:

$$\eta_{th} = f(\dot{m}, \Delta T, G) \qquad (14)$$

The relative uncertainty of the η_{th} results can be expressed as follows:

$$W_{\eta_{th}} = \left[\left(\frac{\partial \eta_{th}}{\partial \dot{m}} W_{\dot{m}}\right)^2 + \left(\frac{\partial \eta_{th}}{\partial \Delta T} W_{\Delta T}\right)^2 + \left(\frac{\partial \eta_{th}}{\partial G} W_G\right)^2\right]^{\frac{1}{2}} \qquad (15)$$

The uncertainties of measured and resulting data are illustrated in Table 4.

Table 4. Uncertainties of measured and resulting data.

Parameter	Uncertainty
Temperature of air (ºC)	±1.5
Mass flow rate (kg/s)	±0.03
Solar radiation (W/m²)	±1.5
Efficiency (%)	±2.5

3. Result and Discussion

3.1. Performance of the SAH Without PCM

Three different arrangements for the solar air heater, as well as a flat plate case integrated with and without PCM and flow turbulators, are investigated experimentally in February and March 2023 under Baghdad city climatic conditions. The SAH arrangements include airflow turbulators incorporated with the absorber plate in V-shaped, cylindrical vertical, cylindrical horizontal, and flat configurations, without turbulators. Variation of inlet, outlet, absorber plate temperatures, and the difference between inlet and outlet temperatures for the SAH without PCM for different cases are shown in Figs. 7, 8, 9, and 10. The variation in the solar radiation during the SAH testing period is also illustrated in these figures. It can be observed that the air and absorber plate temperatures increase with time due to the irradiance increasing, and the maximum values were at a relatively lower air flow rate of 0.002 kg/s during a peak solar radiation period at hour 13.0. Average temperature of the SAH absorber plate was 54.5, 43.9, 46.9, and 50.5 °C for the cases of flat plate, V-shape, circular-shape-vertical, and circular-shape-horizontal, respectively. The SAH with a V-shape flow turbulator had reflected a lower plate temperature due to the enhancement in the heat exchange with the air in this case, compared to other flow turbulators (circular-shape-vertical and circular-shape-horizontal). This behavior in the results can be obviously explained in Fig. 11, which shows the variation of outlet air temperature with time for different testing cases of SAH without PCM. The maximum air outlet temperature was about 43, 38.5, 37, and 35.5 ºC for the flow turbulators cases 1, 2, 3, and flat plate, respectively. It can be observed that the outlet air temperature for the SAH at case 1 of flow turbulators was higher by about 11.7, 16, and 21% compared to cases 2, 3, and the flat plate, respectively. The turbulence in the air flowing in the SAH channel at case 1 was higher, resulting in an enhancement in the heat exchange between the air and the absorber plate and a significant rise in the air outlet temperature. A similar trend in the outlet air temperature results can be seen in Fig. 12**,** which shows the variation of outlet air temperature with air flow rate for different testing cases of SAH without PCM. The outlet air temperature decreased with increasing air flow rate. This behavior can be explained based on energy balance in the SAH, where, at a specified heat gain from the absorber plate, the air with a lower flow rate is highly affected by the heat compared with other flow rates. The variation of thermal efficiency with time for different testing configurations of SAH without PCM is depicted in Fig. 13. From the definition of the thermal efficiency, the SAH at a relatively greater air flow rate of 0.012 kg/s has revealed higher thermal efficiency. The average thermal efficiency of the SAH was about 65, 52, 38, and 30% for cases 1, 2, 3, and the flat plate, respectively.

3.2. Performance of the SAH With PCM

Performance evaluation of the solar air heater integrated with PCM at different SAH configurations with and without flow turbulators is explained in Figs. 14, 15, and 16. Incorporating phase change material (Paraffin wax) as a thermal storage system with the SAH absorber plate will contribute to storing the excess heat of solar radiation during peak sunshine hours. This heat gained by PCM is released into the air passing through the SAH channel during a low solar radiation period. Therefore, the duration of the SAH operation can be extended, and the energy used for space heating can be saved. Investigating the experimental results in the previous section reflects relatively higher performance for the SAH arrangement with the V-shape flow turbulator (case 1). Variation in temperatures of the air inlet, air outlet, absorber plate, and PCM, with time for SAH with PCM at case 1 and ṁ=0.002 kg/s, is shown in Fig.14. As discussed previously, a lower air flow rate has shown a higher temperature distribution in the SAH air channel and PCM compared with other air flow rates.

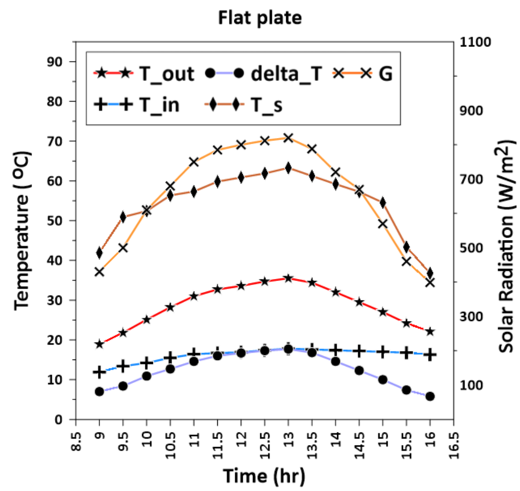

Figure 7. Variation of temperature and solar radiation with time for SAH with a flat plate at ṁ= 0.002 kg/s.

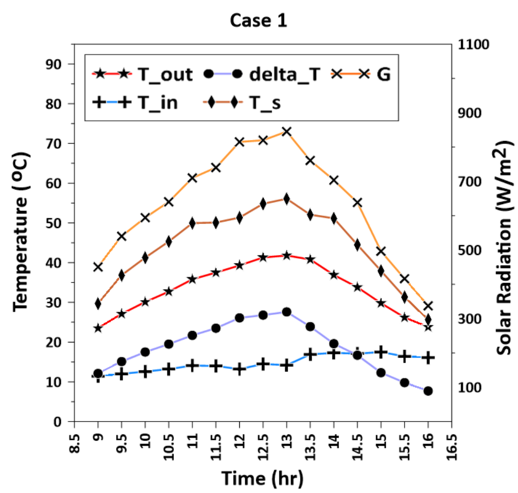

Figure 8. Variation of temperature and solar radiation with time for SAH at case 1 (V-shape) and ṁ= 0.002 kg/s.

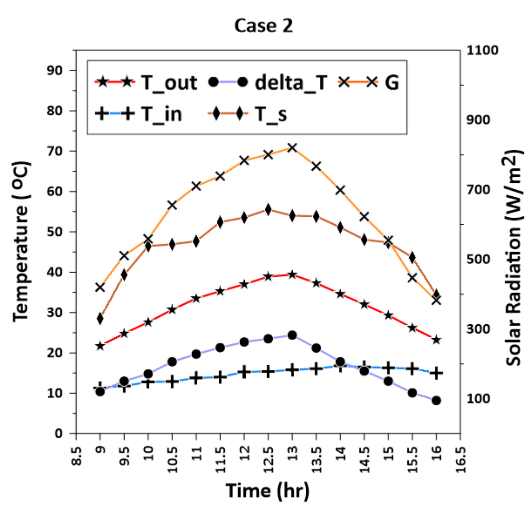

Figure 9. Variation of temperature and solar radiation with time for SAH at case 2 (circular shape-vertical) and ṁ= 0.002 kg/s.

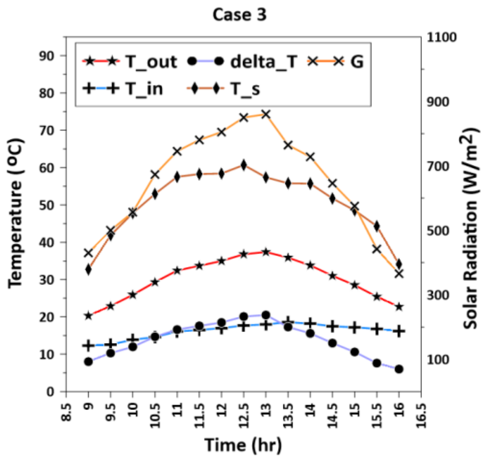

Figure 10. Variation of temperature and solar radiation with time for SAH at case 3 (circular shape-horizontal) and ṁ= 0.002 kg/s.

Fig.15 illustrates the variation of outlet air temperature with time for different testing cases of SAH with PCM at a flow rate of 0.002 kg/s. It can be noticed that as the solar radiation increases, the air temperature also increases over time. The highest temperature was recorded during peak irradiance at hour 13.0. Among the three cases studied, SAH (with a V-shaped turbulator) had the highest outlet air temperature. It was about 4%, 7%, and 12% higher than the temperature of cases 2, 3, and the flat plate, respectively. The variation in energy saving of PCM during the charging and discharging cycles of the PCM at different testing cases and flowrate 0.005 kg/s is depicted in Fig.16. The energy saving represents the excess heat stored in the PCM during charging cycle at peak solar radiation period, and released at low solar radiation in the discharging cycle beyond the hour 14.0. Maximum heat stored by the PCM (energy saving) was 900, 930, 950, and 1040 kJ for the flow turbulator cases 1, 2, and 3, and the flat absorber plate, respectively. The SAH arrangements with the flow turbulators in cases 1, 2, and 3 demonstrated lower heat storage compared to a flat plate. The reason for this outcome is the turbulence effect in the airflow, which improves the heat transfer between the absorber plate and air, resulting in a decrease in the amount of heat transferred to the PCM.

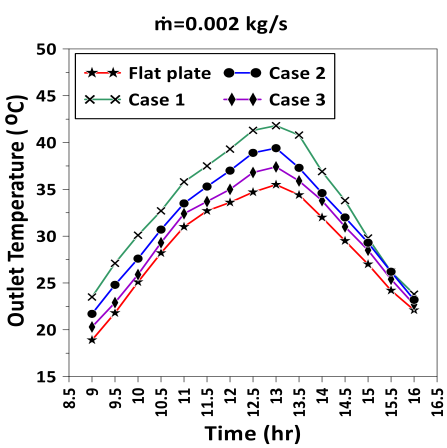

Figure 11. Variation of outlet air temperature with time for different testing cases of SAH without PCM.

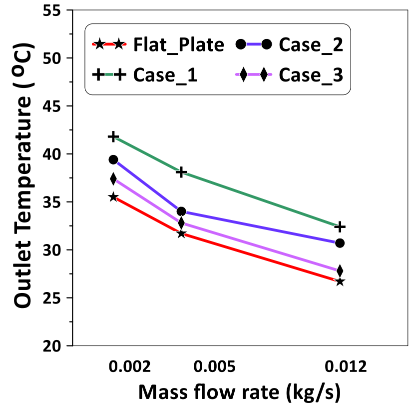

Figure 12. Variation of outlet air temperature with air flow rate for different testing cases of SAH without PCM.

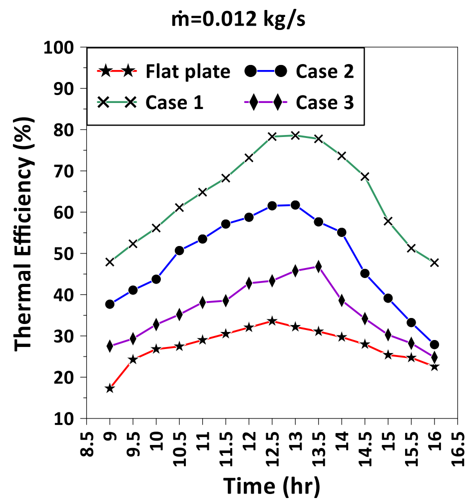

Figure 13. Thermal efficiency as a function of time for different testing configurations of SAH without PCM.

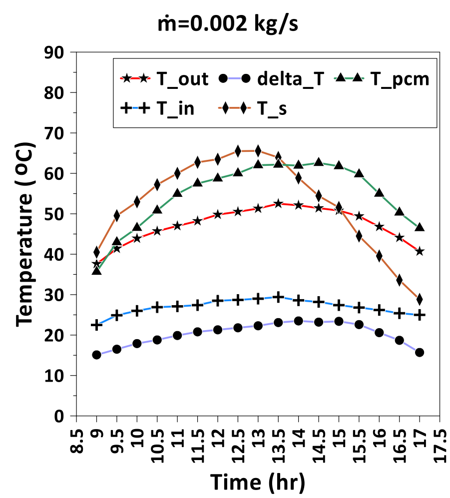

Figure 14. Variation of temperatures with time for SAH with PCM at case 1 (V-shaped flow turbulators) and ṁ=0.002 kg/s.

3.3. Effect of Flow Turbulators and PCM on SAH Performance

To study the effect of flow turbulators and the integration of PCM with a solar air heater setup on the thermal performance of the SAH, the results of outlet air temperature, sound energy, and thermal efficiency are compared in two cases: one without turbulators and PCM, and the other with turbulators and PCM. The comparison of the SAH sound energy and thermal efficiency results is demonstrated in Figs. 17 and 18, respectively.

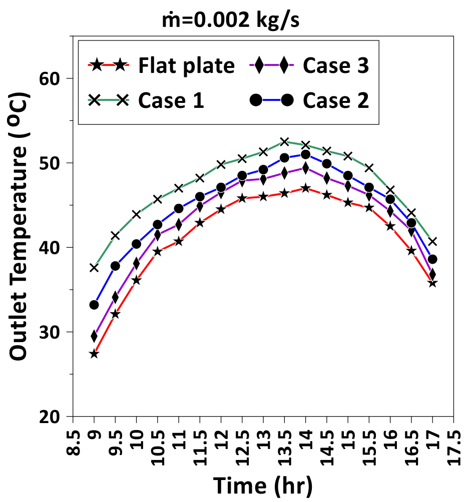

Figure 15. Variation of outlet air temperature with time for different testing cases of SAH with PCM at a flow rate of 0.002 kg/s.

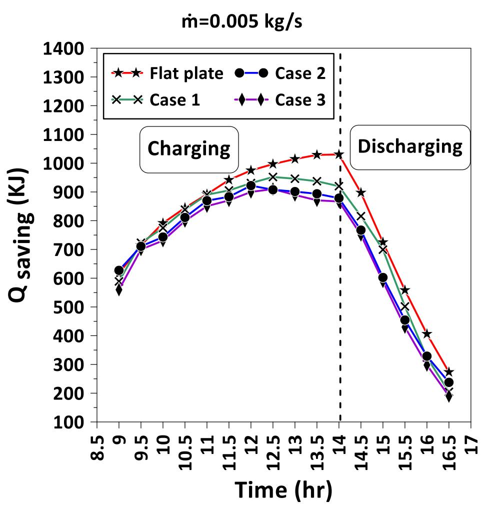

Figure 16. Energy saving of PCM during the charging and discharging cycles of the PCM at different testing cases and a flow rate of 0.005 kg/s.

Fig.17 demonstrates the comparison of the valuable energy supplied to the air for SAH with and without PCM and flow turbulators at an air flow rate of 0.005 kg/s. It can be noticed that, during the PCM discharging period after 14.0 hours at relatively low solar radiation, the SAH arrangement with flow turbulators and PCM reflected a higher sound energy. The useful energy supplied by modified SAH with flow turbulators and PCM in cases 1, 2, and 3 was greater than conventional SAH by about 27, 16, and 9% respectively. While the comparison of the thermal efficiency of SAH at an air flow rate of 0.005 kg/s had reflected a higher efficiency for SAH arrangements with flow turbulators, as shown in Fig.18. As depicted in the Figure, the efficiency of SAH with PCM and flow turbulators increases significantly during low solar radiation after 14:00 due to the effect of heat release by PCM. This heat is added to the solar radiation energy during the discharging cycle, when the efficiency is determined based on the thermal efficiency equation (11). The modified SAH had higher thermal efficiency than the conventional SAH integrated with PCM. Efficiency improvements were 35%, 26%, and 19% for cases 1, 2, and 3 of the modified SAH, respectively.

3.4. Validation of the Present Study Results

The current work results of thermal efficiency at an airflow rate of 0.012 kg/s have been compared with the results reported by Abdulrahman [15], and the comparison is shown in Fig. 19. The solar air heater studied by Abdulrahman did not have flow turbulators and used paraffin wax as a PCM. Thus, the results obtained from the present SAH integrated with PCM and without flow turbulators are compared with Abdulrahman's work. The results indicate a similar trend, with a deviation of around 11%. This deviation in the results can be attributed to some variations in the operating conditions and measurements.

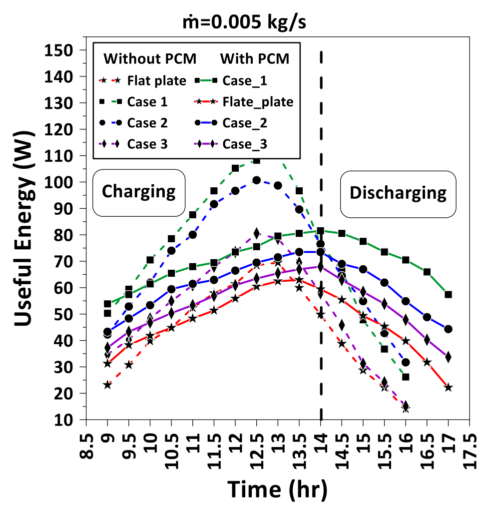

Figure 17. Comparison of the valuable energy for SAH with and without PCM and turbulators at an air flow rate of 0.005 kg/s.

4. Conclusions

The results showed that the modified double-pass SAH has better thermal performance than the conventional SAH, and the Maximum heat stored by the PCM (energy saving) was 900, 930, 950, 950, and 1040 kJ for the flow turbulators V-shaped, cylindrical shaped-vertical, cylindrical shaped-horizontal, and flat absorber plate, respectively. The modified SAH configurations with flow turbulators of V-shaped, cylindrical-shaped vertical, and cylindrical-shaped horizontal showed higher outlet air temperature by about 22, 14, and 9% respectively, compared with the case of a flat plate integrated with PCM. The improvement in modified SAH thermal efficiency was 35%, 26%, and 19% for cases of V-shaped, cylindrical-shaped-vertical, and cylindrical-shaped-horizontal, respectively. It can be concluded that the modified SAH with a V-shaped turbulator resulted in a 22% increase in maximum temperature and an efficiency improvement of 35% compared to the conventional solar air heater.

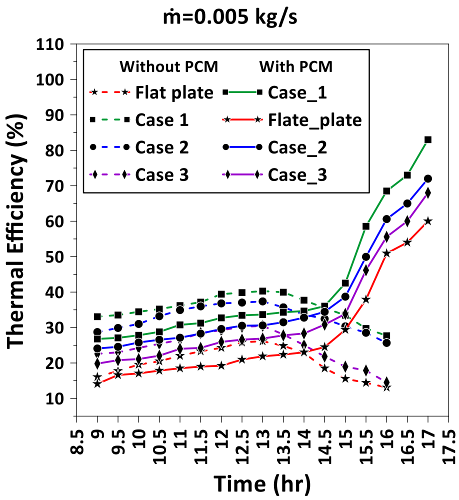

Figure 18. Comparison of the thermal efficiency for SAH with and without PCM and turbulators at an air flow rate of 0.005 kg/s.

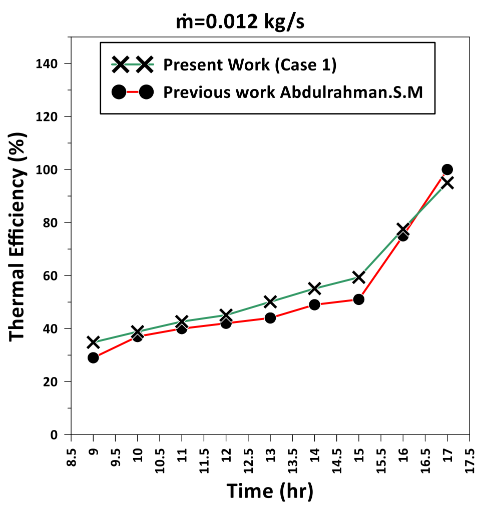

Figure 19. Comparison of the present study results of thermal efficiency with the reported results of Abdulrahman [15].

Acknowledgements

The authors are thankful for the valuable suggestions of the editor and reviewers for improving the quality of the manuscript.

Conflict of interest

The authors declare that there are no conflicts of interest regarding the publication of this manuscript.

Author contributions

Zainab Nadeem: verified the analytical methods, developed the theory, and performed the computations of experimental work.

Ahmed J. Hamad and Abdul Hadi N. Khalifa proposed the research problem and supervised the findings of this work.

Zainab Nadeem and Ahmed J. Hamad: Both authors discussed the results and contributed to the final manuscript.

Nomenclature

A_c: cross-sectional area of the SAH air channel (m^2).

A_s: solar heater absorber plate surface area (m^2).

C_{pa}: air specific heat (J/kg. s).

F_r: heat removal factor for the collector (-)

G: solar irradiance (W/m^2),

$\dot{m}_a$: air mass flow rate (kg/sec).

T_{in}: air inlet temperature (°C).

T_{out}: air outlet temperature (°C)

T_s: absorber plate temperature (°C)

ρ_a: air density (kg/m^3)

α: absorptivity of the absorber plate (-)

τ: transmissivity of the collector glass cover (-)

References

[1] R. K. Srivastava and A. K. Rai, "A review on performance enhancement of solar air heater," Int. J. Mech. Prod. Eng. Res. Dev., vol. 7, no. 5, pp. 279–288, 2017, doi: https://doi.org/10.24247/ijmperdoct201729.

[2] G. Maraba, M. Özerdem, and M. Mobedi, "An experimental study on enhancement of heat transfer in a solar air heater collector by using porous medium," M.S. thesis, Energy Eng., Izmir Inst. Technol., Izmir, Turkey, 2012.

[3] S. Panda and R. Kumar, "A review on heat transfer enhancement of solar air heater using various artificial roughened geometries," J. Adv. Res. Fluid Mech. Therm. Sci., vol. 89, no. 1, pp. 92–133, 2022, doi: https://doi.org/10.37934/arfmts.89.1.92133.

[4] M. K. John, "Analysis of advancement in solar air heater (SAH) heat transfer expansion methods: A crisp review," IOP Conf. Ser.: Mater. Sci. Eng., vol. 1116, no. 1, p. 012050, 2021, doi: https://doi.org/10.1088/1757-899X/1116/1/012050.

[5] Y. Menni, A. Azzi, and A. Chamkha, "A review of solar energy collectors: Models and applications," J. Appl. Comput. Mech., vol. 4, no. 4, pp. 375–401, 2018, doi: https://doi.org/10.22055/JACM.2018.25686.1286.

[6] V. Rajendran et al., "Performance analysis of domestic solar air heating system using V-shaped baffles—An experimental study," Proc. Inst. Mech. Eng. Part E: J. Process Mech. Eng., vol. 235, no. 5, pp. 1705–1717, 2021, doi: https://doi.org/10.1177/09544089211016256.

[7] P. G. Kumar et al., "Performance enhancement of a double-pass solar air heater with a shot-blasted absorber plate and winglets," J. Mech. Sci. Technol., vol. 35, no. 6, pp. 2743–2753, 2021, doi: https://doi.org/10.1007/s12206-021-0544-x.

[8] R. Kumar et al., "Impact of artificial roughness variation on heat transfer and friction characteristics of solar air heating system," Alexandria Eng. J., vol. 61, no. 1, pp. 481–491, 2022, doi: https://doi.org/10.1016/j.aej.2021.06.031.

[9] A. Bekele, M. Mishra, and S. Dutta, "Performance characteristics of solar air heater with surface mounted obstacles," Energy Convers. Manag., vol. 85, pp. 603–611, 2014, doi: https://doi.org/10.1016/j.enconman.2014.04.079.

[10] T. Rajaseenivasan, S. Srinivasan, and K. Srithar, "Comprehensive study on solar air heater with circular and V-type turbulators attached on absorber plate," Energy, vol. 88, pp. 863–873, 2015, doi: https://doi.org/10.1016/j.energy.2015.07.020.

[11] R. Pandey and M. Kumar, “Efficiencies assessment of an indoor designed solar air heater characterized by V baffle blocks having staggered racetrack-shaped perforation geometry,” Sustain. Energy Technol. Assessments, vol. 47, p. 101362, 2021, doi: https://doi.org/10.1016/j.seta.2021.101362.

[12] H. Yaseen, M. Özalp, and W. Khalil, “Second law analysis of double pass solar air heater equipped with aluminum recycled cans as augmentation techniques,” M.S. thesis, Mech. Eng., Karabuk Univ., Turkey, 2022.

[13] A. S. Abdullah et al., “Experimental investigation of single pass solar air heater with reflectors and turbulators,” Alexandria Eng. J., vol. 59, no. 2, pp. 579–587, 2020, doi: https://doi.org/10.1016/j.aej.2020.02.004.

[14] G. Raju and M. M. J. Kumar, “Experimental study on solar air heater with encapsulated phase change material on its absorber plate,” Energy Storage, vol. 3, no. 5, pp. 1–16, 2021, doi: https://doi.org/10.1002/est2.256.

[15] A. S. Mahmood, “Experimental study on double-pass solar air heater with and without using phase change material,” J. Eng., vol. 25, no. 2, pp. 1–17, 2019, doi: https://doi.org/10.31026/j.eng.2019.02.01.

[16] A. Saxena and V. Goel, “Solar air heaters with thermal heat storages,” Chin. J. Eng., vol. 2013, pp. 1–11, 2013, doi: https://doi.org/10.1155/2013/190279.

[17] H. M. Ali, A. I. Bhatti, and M. Ali, “An experimental investigation of performance of a double pass solar air heater with thermal storage medium,” Therm. Sci., vol. 19, no. 5, pp. 1699–1708, 2015, doi: https://doi.org/10.2298/TSCI140824140A.

[18] T. K. Abdelkader et al., “Energy and exergy analysis of a flat-plate solar air heater artificially roughened and coated with a novel solar selective coating,” Energies, vol. 13, no. 4, 2020, doi: https://doi.org/10.3390/en13040997.

[19] Z. Alabdeen H. Obaid, A. Al-damook, and W. H. Khalil, “The thermal and economic characteristics of solar air collectors with different delta turbulators arrangement,” Heat Transf. - Asian Res., vol. 48, no. 6, pp. 2082–2104, 2019, doi: https://doi.org/10.1002/htj.21472.

[20] N. F. Hussein, S. T. Ahmed, and A. L. Ekaid, “Thermal performance of double pass solar air heater with tubular solar absorber,” Int. J. Renew. Energy Dev., vol. 12, no. 1, pp. 11–21, 2023, doi: https://doi.org/10.14710/ijred.2023.46328.

[21] S. Panda and R. Kumar, “A review on heat transfer enhancement of solar air heater using various artificial roughened geometries,” J. Adv. Res. Fluid Mech. Therm. Sci., vol. 89, no. 1, pp. 92–133, 2022, doi: https://doi.org/10.37934/arfmts.89.1.92133.

[22] M. Aktaş et al., "Energy-exergy analysis of a novel multi-pass solar air collector with perforated fins," Int. J. Renew. Energy Dev., vol. 8, no. 1, pp. 47-55, 2019, doi: https://doi.org/10.14710/ijred.8.1.47-55.

[23] H. F. Oztop, F. Bayrak, and A. Hepbasli, “Energetic and exergetic aspects of solar air heating (solar collector) systems,” Renew. Sustain. Energy Rev, vol. 21, pp. 59–83, 2013, doi: https://doi.org/10.1016/j.rser.2012.12.019.

[24] B. Varun Kumar et al., “A performance evaluation of a solar air heater using different shaped ribs mounted on the absorber plate—A review,” Energies, vol. 11, no. 11, 2018, doi: https://doi.org/10.3390/en11113104.

[25] K. I. Al-Chlaihawi, B. H. Alyas, and A. A. Badr, “CFD based numerical performance assessment of a solar air heater duct roughened by transverse-trapezoidal sectioned ribs,” Int. J. Heat Technol., vol. 41, no. 5, pp. 1273–1281, 2023, doi: https://doi.org/10.18280/ijht.410517.

[26] B. K. Roomi and M. A. Theeb, “Experimental and numerical study of inserting an internal hollow core to finned helical coil tube-shell heat exchanger,” J. Eng. Sustain. Dev., vol. 25, no. 1, pp. 1–14, 2021, doi: https://doi.org/10.31272/jeasd.25.1.1.

[27] F. Chabane, N. Moummi, and A. Brima, “Experimental study of thermal efficiency of a solar air heater with an irregularity element on absorber plate,” Int. J. Heat Technol., vol. 36, no. 3, pp. 855–860, 2018, doi: https://doi.org/10.18280/ijht.360311.

[28] J. Hu et al., “Numerical analysis of mechanical ventilation solar air collector with internal baffles,” Energy Build., vol. 62, pp. 230–238, 2013, doi: https://doi.org/10.1016/j.enbuild.2013.03.015.

[29] E. A. Handoyo et al., “Numerical studies on the effect of delta-shaped obstacles’ spacing on the heat transfer and pressure drop in v-corrugated channel of solar air heater,” Sol. Energy, vol. 131, pp. 47–60, 2016, doi: https://doi.org/10.1016/j.solener.2016.02.031.

[30] A. E. Kabeel et al., “Influence of fin height on the performance of a glazed and bladed entrance single-pass solar air heater,” Sol. Energy, vol. 162, pp. 410–419, 2018, doi: https://doi.org/10.1016/j.solener.2018.01.037.

[31] A. J. Hamad, F. M. Hussien, and J. Faraj, “Multiple phase change materials for performance enhancement of a solar dryer with double pass collector,” Energy Eng., vol. 118, no. 5, pp. 1483–1497, 2021, doi: https://doi.org/10.32604/EE.2021.016867.

[32] M. S. Aiswarya and C. R. Divya, “Economic analysis of solar dryer with PCM for drying agricultural products,” Int. Res. J. Eng. Technol., vol. 2, no. 4, 2015.

[33] W. Youssef, Y. T. Ge, and S. A. Tassou, “CFD modelling development and experimental validation of a phase change material (PCM) heat exchanger with spiral-wired tubes,” Energy Convers. Manag., vol. 158, pp. 498–510, 2018, doi: https://doi.org/10.1016/j.enconman.2017.12.075.

[34] A. J. Hamad, “Energy saving and charging discharging characteristics of multiple PCMs subjected to internal air flow,” Fluids, vol. 6, no. 8, p. 275, 2021, doi: https://doi.org/10.3390/fluids6080275.

[35] H. W. Coleman and W. G. Steele, Experimentation, Validation, and Uncertainty Analysis for Engineers, 3rd ed. Hoboken, NJ, USA: Wiley, 2018.